ARMA 22–277

Microbially Induced Calcite Precipitation for Sealing Anhydrite Fractures with Gouges

Guijie Sang, Rebecca J. Lunn, James M. Minto, Grainne El Mountassir
Department of Civil and Environmental Engineering, University of Strathclyde, Glasgow, UK

ABSTRACT: Caprock formation forms a natural barrier for geological storage of CO_2, nuclear wastes, and hydrocarbon resources. Fault and natural/artificial fractures that crosscut the storage systems represent potential leakage pathways. Sealing of caprock fractures/faults is of great importance to ensure its long-term sealing integrity. In this study, we conduct microbial-induced-calcite-precipitation (MICP) experiments for sealing anhydrite fractures (artificially cut) with gouges. MICP involves a bio-chemical reaction for calcite precipitation using ureolytic microorganism - *Sporosarcina pasteurii*. The precipitated calcite, which occurs initially from finer pores to larger pores, induces a 10.7% decrease of porosity inside the fracture after the 1st 12 cycles of MICP treatment. After 18-21 cycles of MICP treatment, the fracture permeability of the two fractured core samples effectively decreases by 2-3 orders of magnitude. Our study also indicates that the MICP sealing efficiency could be improved by lowering the injection rate, optimizing fluid chemistry for a better bacteria retention inside the fracture. The study provides a baseline for using MICP technique to seal anhydrite fractures.

1. INTRODUCTION

Caprocks with very low permeability and ultra-fine pores, consisting of massive consolidated clay-rich sediments (shale) and evaporites such as anhydrite and halite, create natural barriers for hydrocarbon resources, CO_2 sequestration, disposal of radioactive wastes, hydrogen storage, etc. However, natural fractures/faults or injection-induced fractures that crosscut subsurface storage systems (Figure 1) could provide potential leakage pathways [1,2]. Seeking an efficient technique to seal caprock fractures is crucial.

Microbially induced calcite precipitation (MICP) has been considered as an environmentally sustainable grouting technology for soil improvement [3,4], fracture sealing [5–8], removal of contaminants in ground water [9,10], among others. It has several advantages over conventional cement grouting methods, including (1) the low viscosity of the bacterial solution and cementing solution (urea and calcium chloride), which allows to penetrate with relatively low pumping power; (2) micron-size microbes for sealing fine pores and fractures; and (3) potential low carbon footprint. MICP is a naturally occurring metabolic phenomenon that can be found in soil and marine environment [11]. This bio-inspired grouting technique also have advantages over conventional chemical grouting method (such as acrylates, acrylamides, and polyurethanes, *etc*.) due to its lower cost of the raw materials and less toxicity to the environment [12].

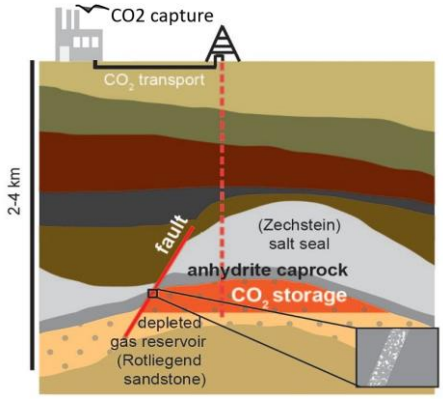

Figure 1. Caprock for CO_2 storage in the North Sea [13].

The most commonly utilized bacteria for MICP are alkali-tolerant ureolytic microorganisms, which decomposes urea into carbonate ion and ammonium *via* the production of urease enzyme, as shown in Equation (1). This results in a local increase in pH and precipitation of calcium carbonate if calcium is available - as described in Equation (2). The growth of the calcium carbonate around the microorganism finally forms calcite crystals [14] and effectively acts as nucleation sites for sealing and bonding porous and fractured media.

$$CO(NH_2)_2 + 2H_2O \xrightarrow{urease} 2NH_4^+ + CO_3^{2-} \quad (1)$$

$$Ca^{2+} + CO_3^{2-} \rightarrow CaCO_3 \downarrow \quad (2)$$

There has been an increasing interest in using MICP to treat porous/fractured rocks in both laboratory [8,15–17] and field scale [6,18]. However, to our best knowledge, there is still lack of experimental evidence of using MICP to seal anhydrite fractures, which could potentially cause CO_2 leakage if acting as caprock formation as schematically shown in Figure 1. Since bacterial transport and retention behaviors are highly dependent on the physico-chemical characteristics of the rock fractures and fluids chemistry [19,20], it is still an enigma for an effective calcite precipitation along anhydrite fractures. Our study aims at evaluating the viability of application of MICP for the sealing of anhydrite fractures and provide potential treatment strategies for caprock sealing.

2. EXPERIMENTAL METHODS

2.1. Rock samples and experimental setup

The anhydrite samples were originally collected from West Midlands, UK. The specimens are a pale grey or white color exhibiting a relatively soft hardness and crystalline texture. As shown in Figure 2, two core samples #1 and #2 (diameter: ~19 mm; length: ~ 45 mm) were prepared with an artificially-cut fracture in the middle. Mounted inside the fracture were 1-2 layers of anhydrite particles, with their size ranging from 212 µm to 425 µm to represent the fault gouges. Based on X-ray CT scans, the sample dimensions were determined in Table 1. Specifically, the fracture apertures for the two samples were 0.59 mm and 0.73 mm, respectively. Meanwhile, the pore volume of the porous gouges inside the fractures of the sample #1 was 0.256 ml, with its porosities being 48.6%. The pore volume and porosity of sample #2 were unquantified due to the similar X-ray attenuations of anhydrite and the precipitated calcite.

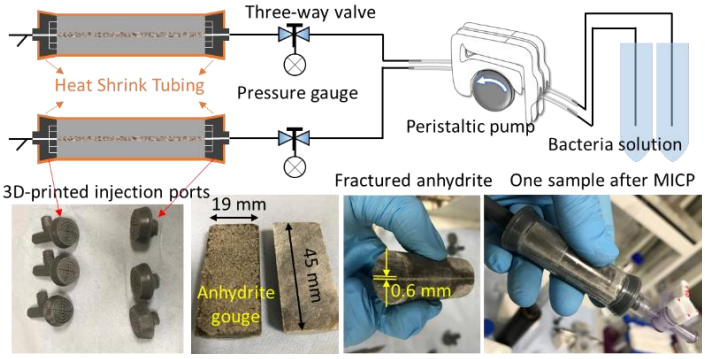

Figure 2. Experimental setup of the MICP treatment for sealing artificially-cut fracture of anhydrite samples. Anhydrite particles (212-425 µm) were mounted inside the fracture to represent fault gouges.

The experimental setup is also schematically shown in Figure 2, which consisted of a solution source (bacteria solution, urea & $CaCl_2$ solution), a peristaltic pump, a pressure gauge and an injection system. The injection system comprised a fractured anhydrite core and a set of 3-D printed ports (inlet and outlet), which were confined by a clear heat shrink sleeve capable of providing a fairly amount of confining stress so as to avoid leakage along the sample wall.

Table 1. Fracture dimension and parameters of porous gouges inside the fracture based on X-ray CT results.

#	Fracture dimension			Gouge	
	Length	Width	Aperture	Pore Volume	Porosity
	mm	mm	mm	ml	-
#1	45.87	19.44	0.59	0.256	0.486
#2	45.97	19.37	0.73	unknown *	unknown *

* Sample #2 were scanned with X-ray CT only after the MICP treatment. The initial pore volume and porosity of sample #2 were unquantified due to the similar X-ray attenuations of anhydrite and the precipitated calcite, making the two solids hard to be segmented.

2.2. Bacteria culture

In this study, the ureolytically active bacterium *Sporosarcina pasteurii* was used. The bacteria were cultured in the autoclaved yeast extract media supplemented with the filtered urea (20 g/L) solution. Cultures were incubated in a shaker-incubator at 30 °C and 115 rpm over a period of 24 hours. The cells were harvested by centrifugation at a speed of 6000g for 8 minutes. Then the centrifuged bacteria were re-suspended into designated solution (i.e., deionized water and 0.05 M $CaCl_2$) to achieve a desired optical density (OD_{600} approximately 1.0), which was determined by a UV-VIS spectrophotometer at a wavelength of 600 nm. The specific urease activity of the bacteria, defined as the amount of urease activity per unit biomass, was determined using the conductivity method [21]. The rate of changes in electrical conductivity (µS/cm/min) was converted to the rate of changes in urea concentration (mM/min) using the conversion factor of 10.62 [7]. The average specific urease activity of the bacteria for the MICP treatment were determined as 2.65 (standard deviation: 0.68).

2.3. MICP treatment strategy and permeability test

There were two stages for the MICP experiment. In the first stage, 12 cycles of MICP grouting were performed with each cycle per day. For each cycle, two sets of 0.5 ml (~2 pore volumes) bacterial solutions, one in deionized water and the other in 0.05 M $CaCl_2$ fixer (which encourages bacteria flocculation [8,16]), were injected respectively into the two fractured core samples (#1, #2) at a flow rate of 1.0 ml/min. This was followed by an hour static time for bacteria settlement. Afterwards, 0.5 ml cementing solution (1 M urea & 1 M $CaCl_2$) was injected into the two fractured core samples at the same flow rate

(i.e., 1.0 ml/min). The reaction time was around 23 hours till next cycle.

After each cycle, the permeability test was conducted using deionized water. The permeability of the fracture with gouges k_f was determined by Darcy's law given by the following equation.

$$k_f = \frac{qL\mu}{A_f \Delta p} \quad (3)$$

where q (m^3/s) is the flow rate; L (m) is the length of the fracture; A_f (m^2) is the cross-sectional area of the fracture, which is the product of fracture width and aperture; ΔP (Pa) is the differential pressure between inlet and outlet; μ (Pa·s) is the dynamic viscosity of the solution, which was assumed to be water-like, i.e., 8.9×10^{-4} Pa·s at 25 °C.

The first stage aimed at setting a baseline for using MICP to seal anhydrite samples. In the second stage, we tried to achieve a better sealing with more injection of bacterial and cementing solution. For each cycle, 1.5 ml (~6 pore volume) bacterial solution in deionized water was injected into the two fractured core samples, followed by an hour static time for bacteria settlement. Subsequently, 1.5 ml (~6 pore volume) cementing solution (1 M urea & 1 M $CaCl_2$) was injected with a reaction time of 4 hours, followed by another injection of 1.5 ml cementing solution. The reaction lasted till the next cycle (~19 hours). There were in total 9 treatment cycles for sample #1 and 6 treatment cycles for sample #2 due to the sharp decrease of the permeability which caused a very slow injection of bacterial and cementing solution into the fractured core sample.

2.4. X-ray CT scan

Sample #1 before and after 12 cycles of MICP treatment (stage 1), and sample #2 after 12 cycles of MICP treatment were scanned with a Nikon XT H 225 LC X-ray computed tomography system fitted with 225kV X-ray source and a 3D volume reconstruction using Nikon XTekCT software version 4.3.4. The scanning parameters were 132 kV, 114 µA, 500 milli-second exposure, and 1816 projection (angular step 0.1982 per scan). The spatial resolution of the sample images was 33 µm.

3. EXPERIMENTAL RESULTS

3.1. Decreases in porosity of the gouges in stage 1

One of the X-CT slices of sample #1 before and after 12 cycles of MICP treatment, and one of the slices of sample #2 after 12 cycles of MICP treatment are shown in the right side of Figure 3 and Figure 4, respectively. These data were processed by the FIJI version ImageJ [22]. A binary segmentation (pore spaces and solid particles) was performed based on IsoData thresholding algorithm. The porosity distribution along the fracture length are shown in the left side of Figure 3 and Figure 4, respectively.

After 12 cycles of MICP treatment in stage 1, sample #1 showed a denser particle distribution than that before the MICP treatment (Figure 3), resulting from the calcite precipitation among the gouge particles inside the artificially cut fracture. Before the MICP treatment, the average porosity for all slices normal to the flow direction was 48.6% with a standard deviation of 9.9%. After the treatment, the average porosity for all slices normal to the flow direction was 37.9% (standard deviation: 10.4%). The precipitated calcite induced a decrease of porosity distribution along the whole fracture (Figure 3 left), with its overall porosity reduced by 10.7%. As also shown in Figure 3 (right), calcite precipitation occurs primarily at the smaller pores near gouge particles, leaving larger pores less well bridged. This results from that the bacteria tend to be deposited (1) at particle surfaces through attachment, and (2) at the crevices and constrictions through pore straining, while bacteria suspended in pore fluids are drained during the injection of cementing solution (i.e., 1 M urea & $CaCl_2$). Therefore, the bio-chemical precipitation process starts from finer pores to bigger pores, and gradually seals the fracture.

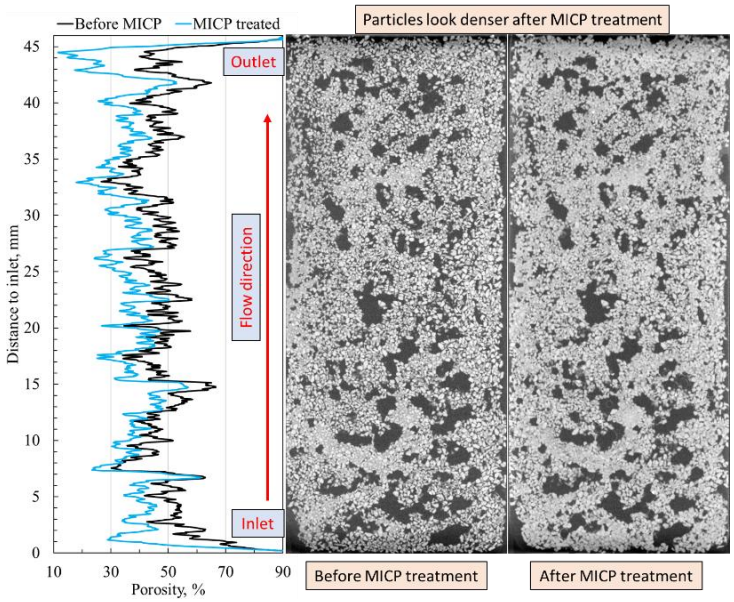

Figure 3. CT images of sample #1 before and after 12 cycles of MICP treatment in Stage 1. The image stack of the fracture was segmented into pore phase and solid phase using Isodata thresholding algorithm. The average porosity of each horizontal slice from bottom to top was obtained accordingly and plotted against the distance to the inlet as shown in the left.

As shown in Figure 4, sample #2 behaved a more scattered distribution of the porosity along the facture length due to the presence of big voids during gouge packing. After 12 cycles of MICP treatment, the average porosity for all slices normal to the flow direction was also 37.9% with a standard deviation of 15.4%. Figure 4 also presents a gray-shaded region in the big voids with its distance to the inlet being 17 mm. This could be the undrained pore fluids mixed with calcium carbonate without being crystallized.

Compared to sample #1 which was treated using bacteria suspended in deionized water, samples #2 was treated using bacteria suspended in 0.05 M $CaCl_2$ (as a fixer) in stage 1. The fixer could enhance the bacteria flocculation and hence bacterial straining at pore crevices and constrictions. After 12 cycles of MICP treatment, sample #2 presented a denser particle distribution at the near inlet region than that at the near outlet region (Figure 4), possibly resulting from the enhanced bacteria straining near inlet region.

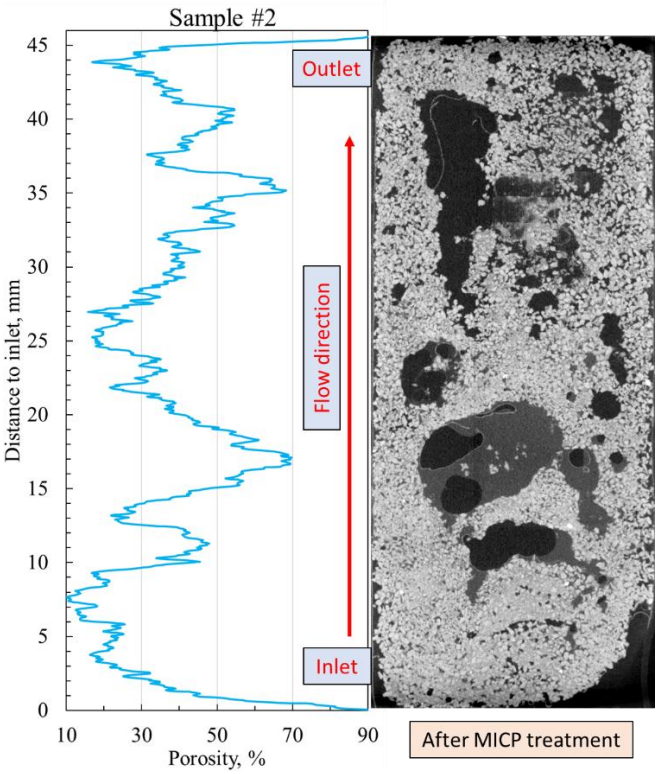

Figure 4. CT image of sample #2 after 12 cycles of MICP treatment in Stage 1. The image stack of the fracture was segmented (pore and solid phases) using Isodata thresholding algorithm, with the average porosity of each horizontal slice plotted at the left.

3.2. Evolution of fracture permeability

The evolutions of the fracture permeability of the two fractured core samples are shown in Figure 5. The fracture permeability decreased by one order of magnitude after stage 1, and decreased by 2-3 orders of magnitude after stage 2. During stage 1 with the injection of ~2 pore volumes of bacterial and cementing solution for each cycle, the fracture permeability gradually decreased with more MICP treatment cycles, and tended to be stable after the 9th cycle. The initial faster decreases in fracture permeability of the two fractured core sample (#1, #2) can be attributed to a faster calcite precipitation at finer pores as shown in Figure 3 and Figure 4. As finer pores were gradually filled with the precipitated calcite (porosity decreased accordingly), local velocity at the finer pores kept increasing, making it hard for bacterial attachment due to higher hydrodynamic shear forces. Meanwhile, a gradual calcite precipitation in bigger voids (preferential flow channel) caused a slow decrease in the overall permeability of the fracture. This phenomenon resonates well with the previous study by (El Mountassir et al., 2014) [5] that feedback mechanism exists between the gradual reduction in fracture aperture due to precipitation, and its effect on the local fluid velocity, causing preferential flow channels inside the fracture.

The two fractured cores behaved almost same permeability in Stage 1. This is consistent with the same overall porosity after 12 cycles of MICP treatment as mentioned in the last section. Despite the similar overall fracture porosity and permeability for the two samples after 12 cycles of MICP treatment, sample #2 (bacteria suspended in 0.05 M $CaCl_2$) presented more calcite precipitation near the inlet due to higher bacterial straining, while sample #1 (bacteria suspended in deionized water) presented a relatively homogeneous calcite precipitation in fine pores along the fracture length.

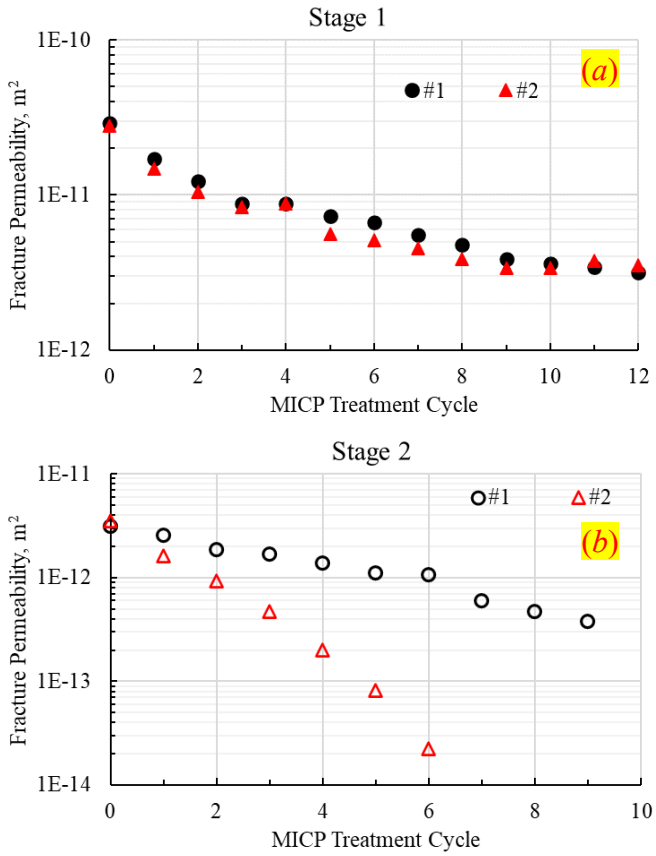

Figure 5. Evolution of fracture permeability with the increase of MICP treatment cycles in stage 1 (*a*) and stage 2 (*b*).

In stage 2 with the injection of ~6 pore volumes of bacterial and ~12 pore volumes of cementing solution for each cycle, sample #1 presented a continuous decrease in fracture permeability as the treatment cycle increased. As expected, the decrease in fracture permeability in stage 2 was faster than that in stage 1 due to more injection of bacteria and cementing solution. Sample #2 presented a faster decreasing trend than sample #1, resulting possibly

from a quick calcite precipitation (clogging) in the near inlet region due to more injection of bacteria and cementing solutions.

4. DISCUSSION AND POTENTIAL TREATMENT STRATEGY FOR FRACTURE SEALING

Calcite precipitation in porous fractured media by ureolytic bacteria is highly influenced by many bio-physico-chemical factors including bacterial density, urease activity, ionic strength, pore/fracture morphology, surface charge, flow rate, pH, temperature, etc. Specifically, these physico-chemical factors control bacterial transport and retention in the porous fractured media, which in turn affect the bio-chemical reactions and hence the flow behavior. In this section, we will discuss some key external factors (such as flow rate and fluid chemistry) that influence the sealing efficiency of anhydrite fractures based on our experimental results above.

During MICP treatment in stage 1, calcite precipitation gradually fills in finer pores, inducing an enhancement of the local pore (seepage) velocity. For example, the Darcy velocity in the artificially cut fracture of sample #1 (cross-sectional area: 11.47 mm^2) under a flow rate of 1.0 ml/min was calculated to be 8.7 cm/min. After 12 cycles MICP treatment, the overall porosity of sample #1 decreased from 48.6% to 37.9%, corresponding to an increase in the overall seepage velocity from 18 cm/min to 23 cm/min. This caused a lower bacteria attachment due to the higher hydrodynamic force, and hence a slower decrease in overall fracture permeability as MICP cycles proceeded. Therefore, a slower injection rate could potentially promote a more efficient fracture sealing.

Meanwhile, the use of 0.05 M $CaCl_2$ enhances the bacterial flocculation. In this sense, adding a proper amount of $CaCl_2$ into bacteria solution contributes to a better deposition of the bacteria through pore straining and hence promotes fracture sealing efficiency. However, it should be noted that too much bacteria flocculation may cause clogging near the inlet. It is important to find an optimized fluid chemistry in which the bacteria can be more homogeneously deposited in the gouge surfaces and/or pore throats along the fracture.

As expected, more injection of bacterial and cementing solution promoted to the fracture sealing as shown in Figure 5 (*b*). However, this costs more materials and causes a big waste. As a matter of fact, in stage 2 with the injection of ~6 pore volumes of bacterial solution (in deionized water) and ~12 pore volumes of cementing solution for each cycle, most of the bacteria were drained away without effectively attached at gouge surfaces or strained at pore throats. The cementing solution were also not well utilized by the bacteria due to the limited interaction space. In the future, it is necessary to first find a proper fluid chemistry for better bacterial retention along the fracture. Meanwhile, a new injection strategy needs to be found out to make the full use of cementing solution (i.e., urea and $CaCl_2$). For example, during each cycle, instead of pumping a large volume of cementing solution once or twice, pumping only one pore volume of cementing solution followed by a continuous supply with a very slow injection rate may achieve a better fracture sealing efficiency, in which case the consumption of the raw materials could be lower.

5. CONCLUSION

MICP experiments on artificially cut anhydrite fractures with gouges were conducted in this study. Some major conclusions are summarized as follows.

(1) After 12 cycles of MICP treatment in stage 1 and 6-9 cycles of MICP treatment in stage 2, the fracture permeability declined by 2-3 orders of magnitude due to calcite precipitation;

(2) Calcite precipitation occurred initially at fine pores and effectively reduced the overall porosity. This in turn increased seepage velocity in local pores and potentially caused a lower bacteria attachment due to higher hydrodynamic shear forces.

(3) 0.05 M $CaCl_2$ solution as a fixer could enhance bacteria deposition, but it may also cause a faster calcite precipitation near the injection region.

(4) For a better sealing efficiency, future treatment strategy should consider lowering the injection rate, choosing a better fluid chemistry, and making a better use of cementing solution.

ACKNOWLEDGEMENTS

This study was funded internally by the University of Strathclyde (21/22 StrathWide – Project 2).

REFERENCES

(1) Pluymakers, A. M. H.; Samuelson, J. E.; Niemeijer, A. R.; Spiers, C. J. Effects of Temperature and CO_2 on the Frictional Behavior of Simulated Anhydrite Fault Rock. *J. Geophys. Res. Solid Earth* **2014**, *119* (12), 8728–8747. https://doi.org/10.1002/2014JB011575.

(2) Pluymakers, A. M. H.; Niemeijer, A. R. Healing and Sliding Stability of Simulated Anhydrite Fault Gouge: Effects of Water, Temperature and CO2. *Tectonophysics* **2015**, *656*, 111–130. https://doi.org/10.1016/j.tecto.2015.06.012.

(3) Gomez, M. G.; Martinez, B. C.; DeJong, J. T.; Hunt, C. E.; deVlaming, L. A.; Major, D. W.; Dworatzek, S. M. Field-Scale Bio-Cementation Tests to Improve Sands. *Proc. Inst. Civ. Eng. - Gr. Improv.* **2015**, *168* (3), 206–216. https://doi.org/10.1680/grim.13.00052.

(4) El Mountassir, G.; Minto, J. M.; van Paassen, L. A.; Salifu, E.; Lunn, R. J. Applications of Microbial Processes in Geotechnical Engineering. *Adv. Appl. Microbiol.* **2018**, *104*, 39–91. https://doi.org/10.1016/BS.AAMBS.2018.05.001.

(5) El Mountassir, G.; Lunn, R. J.; Moir, H.; MacLachlan, E. Hydrodynamic Coupling in Microbially Mediated Fracture Mineralization: Formation of Self-Organized Groundwater Flow Channels. *Water Resour. Res.* **2014**, *50* (1), 1–16. https://doi.org/10.1002/2013WR013578.

(6) Phillips, A. J.; Cunningham, A. B.; Gerlach, R.; Hiebert, R.; Hwang, C.; Lomans, B. P.; Westrich, J.; Mantilla, C.; Kirksey, J.; Esposito, R.; et al. Fracture Sealing with Microbially-Induced Calcium Carbonate Precipitation: A Field Study. *Environ. Sci. Technol.* **2016**, *50* (7), 4111–4117. https://doi.org/10.1021/acs.est.5b05559.

(7) Minto, J. M.; MacLachlan, E.; El Mountassir, G.; Lunn, R. J. Rock Fracture Grouting with Microbially Induced Carbonate Precipitation. *Water Resour. Res.* **2016**, *52* (11), 8827–8844. https://doi.org/10.1002/2016WR018884.

(8) Tobler, D. J.; Minto, J. M.; El Mountassir, G.; Lunn, R. J.; Phoenix, V. R. Microscale Analysis of Fractured Rock Sealed with Microbially Induced CaCO3 Precipitation: Influence on Hydraulic and Mechanical Performance. *Water Resour. Res.* **2018**, *54* (10), 8295–8308.

(9) Fujita, Y.; Taylor, J. L.; Gresham, T. L. T.; Delwiche, M. E.; Colwell, F. S.; McLing, T. L.; Petzke, L. M.; Smith, R. W. Stimulation Of Microbial Urea Hydrolysis In Groundwater To Enhance Calcite Precipitation. *Environ. Sci. Technol.* **2008**, *42* (8), 3025–3032. https://doi.org/10.1021/ES702643G.

(10) Lauchnor, E. G.; Schultz, L. N.; Bugni, S.; Mitchell, A. C.; Cunningham, A. B.; Gerlach, R. Bacterially Induced Calcium Carbonate Precipitation and Strontium Coprecipitation in a Porous Media Flow System. *Environ. Sci. Technol.* **2013**, *47* (3), 1557–1564.

(11) Boquet, E.; Boronat, A.; Ramos-Cormenzana, A. Production of Calcite (Calcium Carbonate) Crystals by Soil Bacteria Is a General Phenomenon. *Nat. 1973 2465434* **1973**, *246* (5434), 527–529. https://doi.org/10.1038/246527a0.

(12) Ivanov, V.; Chu, J. Applications of Microorganisms to Geotechnical Engineering for Bioclogging and Biocementation of Soil in Situ. *Rev. Environ. Sci. Biotechnol.* **2008**, *7* (2), 139–153. https://doi.org/10.1007/S11157-007-9126-3/TABLES/5.

(13) Pluymakers, A. M. H. Frictional and Sealing Behavior of Simulated Anhydrite Fault Gouge: Effects of CO2 and Implications for Fault Stability and Caprock Integrity. University Utrecht 2015.

(14) Stocks-Fischer, S.; Galinat, J. K.; Bang, S. S. Microbiological Precipitation of CaCO3. *Soil Biol. Biochem.* **1999**, *31* (11), 1563–1571. https://doi.org/10.1016/S0038-0717(99)00082-6.

(15) Mitchell, A. C.; Phillips, A. J.; Hiebert, R.; Gerlach, R.; Spangler, L. H.; Cunningham, A. B. Biofilm Enhanced Geologic Sequestration of Supercritical CO2. *Int. J. Greenh. Gas Control* **2009**, *3* (1), 90–99. https://doi.org/10.1016/j.ijggc.2008.05.002.

(16) Minto, J. M.; Hingerl, F. F.; Benson, S. M.; Lunn, R. J. X-Ray CT and Multiphase Flow Characterization of a 'Bio-Grouted' Sandstone Core: The Effect of Dissolution on Seal Longevity. *Int. J. Greenh. Gas Control* **2017**, *64*, 152–162. https://doi.org/10.1016/j.ijggc.2017.07.007.

(17) Minto, J. M.; Tan, Q.; Lunn, R. J.; El Mountassir, G.; Guo, H.; Cheng, X. 'Microbial Mortar'-Restoration of Degraded Marble Structures with Microbially Induced Carbonate Precipitation. *Constr. Build. Mater.* **2018**, *180*, 44–54. https://doi.org/10.1016/j.conbuildmat.2018.05.200.

(18) Cuthbert, M. O.; McMillan, L. A.; Handley-Sidhu, S.; Riley, M. S.; Tobler, D. J.; Phoenix, V. R. A Field and Modeling Study of Fractured Rock Permeability Reduction Using Microbially Induced Calcite Precipitation. *Environ. Sci. Technol.* **2013**, *47* (23), 13637–13643. https://doi.org/10.1021/es402601g.

(19) Torkzaban, S.; Tazehkand, S. S.; Walker, S. L.; Bradford, S. A. Transport and Fate of Bacteria in Porous Media: Coupled Effects of Chemical Conditions and Pore Space Geometry. *Water Resour. Res.* **2008**, *44* (4). https://doi.org/10.1029/2007WR006541.

(20) Jain, S.; Arnepalli, D. N. Adhesion and Deadhesion of Ureolytic Bacteria on Sand under Variable Pore Fluid Chemistry. *J. Environ. Eng.* **2020**, *146* (6), 04020038. https://doi.org/10.1061/(ASCE)EE.1943-7870.0001708.

(21) Whiffin, V. S. Microbial CaCO3 Precipitation for the Production of Biocement. Murdoch University 2004.

(22) Schindelin, J.; Rueden, C. T.; Hiner, M. C.; Eliceiri, K. W. The ImageJ Ecosystem: An Open Platform for Biomedical Image Analysis. *Mol. Reprod. Dev.* **2015**, *82* (7–8), 518–529. https://doi.org/10.1002/MRD.22489.